Volume 4
Number 10
October 2025
Pages 817–918

Sensors & Diagnostics

rsc.li/sensors

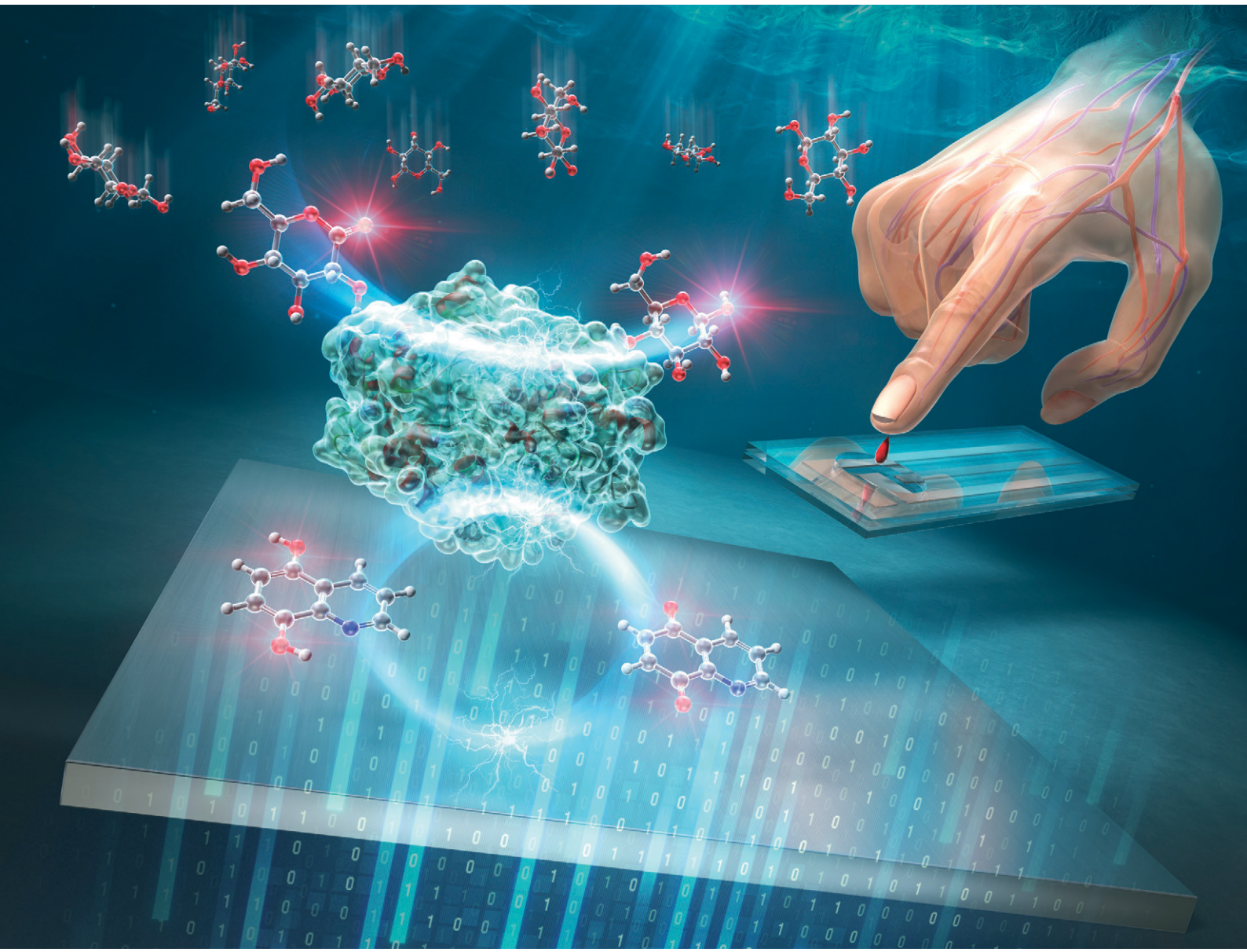

ISSN 2635-0998

ROYAL SOCIETY OF CHEMISTRY

PAPER

Isao Shitanda *et al.*

Insights into the performance-determining aspects of electrochemical biosensor strips by diffusion profile visualization using finite element method simulation

Sensors & Diagnostics

PAPER

View Article Online
View Journal | View Issue

Cite this: *Sens. Diagn.*, 2025, **4**, 839

Insights into the performance-determining aspects of electrochemical biosensor strips by diffusion profile visualization using finite element method simulation

Isao Shitanda, *[ab] Masaki Mizuno,†[a] Noya Loew,†[a] Hikari Watanabe, [a] Masayuki Itagaki[ab] and Seiya Tsujimura [c]

The rate-limiting step in a recently reported glucose sensor strip incorporating a water-soluble quinone mediator with high enzyme reactivity was proposed to be substrate diffusion. This mechanism is expected to lead to sensors requiring smaller mediator amounts but possessing higher sensitivity and a wider measurement range than conventional sensor strips containing mediators with low enzyme reactivity. A general finite element method-based simulation model for mediator-type enzyme electrodes was employed in this study to obtain the concentration distribution profiles of this specific glucose sensor strip and clarify its action mechanism. The obtained profiles showed that the mediator forms a very thin diffusion layer on the electrode surface and that the diffusion layer of the substrate gradually covers the entire solution. The results of this study confirmed that the rate-limiting step of the glucose sensor strip is substrate diffusion.

Received 11th June 2025,
Accepted 26th July 2025

DOI: 10.1039/d5sd00095e

rsc.li/sensors

Introduction

Electrochemical biosensor strips are widely available in the global market in the form of glucose sensor strips for the self-monitoring of blood glucose (SMBG).[1] Blood glucose monitoring is critical for reducing the health hazards associated with diabetes and related diseases.[2–5] The number of patients diagnosed with diabetes mellitus, one of the most common lifestyle-related diseases, is increasing worldwide. Numerous diabetic patients monitor their blood glucose levels daily using SMBG devices (glucose meters) to determine their dietary needs, insulin dosage, and exercise protocol. Consequently, the demand for highly accurate and reliable SMBG devices has steadily increased.

Morshed *et al.* recently developed a glucose sensor strip featuring glucose diffusion as the main performance-controlling process.[6] This strip is characterized by increased sensitivity and an extended linear range, as compared with conventional strips, while requiring only a minimal amount of mediator. The sensor strip includes the commonly utilized enzyme flavin-adenine dinucleotide-dependent glucose dehydrogenase (FAD-GDH), which, unlike glucose oxidase (GOx), is insensitive to molecular oxygen and can maintain high selectivity toward glucose.[7–11] Commercial glucose sensor strips employ ferricyanide or ferrocene derivatives as a mediator,[6,12] prioritizing water solubility over enzyme-mediator reactivity. In contrast to these strips, the strip prepared by Morshed *et al.* employed novel water-soluble quinone derivatives, which have high reactivity toward FAD-GDH.[6]

The difference between classic mediators with poor enzyme reactivity and the new mediator with high enzyme reactivity is best explained using the concept of "reaction layers".[13–15] In systems with a soluble enzyme and mediator, a reaction layer forms at a certain distance from the electrode where the enzymatic reaction occurs. The electrode side of the reaction layer contains a steady supply of the mediator oxidized by the electrode reaction but lacks the substrate. Thus, no enzymatic reaction occurs, and the enzyme is present in its oxidized form. Consequently, the oxidized mediator diffuses into the bulk solution for a certain period until it reaches the reaction layer, where it is reduced by the enzymatic reaction. The reduced mediator then diffuses back to the electrode, where a current is generated by the re-oxidation of the mediator. On the bulk-solution side of the reaction layer, all mediator and enzyme molecules are

[a] *Department of Pure and Applied Chemistry, Faculty of Science and Technology, Tokyo University of Science, 2641 Yamazaki, Noda, Chiba, 278-8510, Japan. E-mail: shitanda@rs.tus.ac.jp*
[b] *Research Institute for Science and Technology, Tokyo University of Science, 2641 Yamazaki, Noda, Chiba 278-8510, Japan*
[c] *Division of Materials Science, Faculty of Pure and Applied Sciences, University of Tsukuba, 1-1-1 Tennodai, Tsukuba, Ibaraki, 305-8573, Japan*
† These authors contributed equally.

reduced; thus, no enzymatic reaction occurs even in the presence of a substrate. The substrate diffuses from the bulk solution to the reaction layer, contributing to the overall reaction mechanism.

The reaction layer in sensor strips containing a mediator with poor enzyme reactivity is located at a significant distance from the electrode, leading to low substrate concentrations. Therefore, mediator diffusion significantly influences the overall turnover and, thus, current response. A large amount of mediator is often used per sensor strip to increase the turnover and response.

Morshed *et al.* reported that the reaction layer in sensor strips with a water-soluble mediator and high enzyme reactivity is likely to be on or close to the electrode surface.[6] Therefore, the reaction turnover and current response are high and mostly independent of mediator diffusion. Given the high turnover, only a small amount of mediator is needed. Furthermore, the overall reaction rate is limited by substrate diffusion and the response current becomes more predictable. These features allow for the preparation of sensor strips with high sensitivity and an extended linear range.[6]

Kitazumi *et al.* employed the reaction-layer concept to construct an analytical model of the enzymatic reactions near microelectrodes.[13] Loew *et al.* also visualized the reaction layers using a general simulation model for mediator-type enzyme electrodes using the finite element method (FEM).[14,15] This model simulated an oxidase or dehydrogenase with a ping-pong bi–bi mechanism, which is the most common type of enzyme in mediator-type enzyme electrodes.

The general FEM model of Loew *et al.*[14] was adapted in this study to the strip-type sensor developed by Morshed *et al.*[6] The general FEM model only considers idealized cases such as both the enzyme and mediator dissolved in a large bulk or both immobilized. The adapted model is more realistic and considers both the geometrical restrictions of a strip-type sensor and the initial enzyme and mediator concentrations near the electrode diffusing into the bulk during the simulation.

This adapted model allowed the diffusion profiles of the strip-type sensor to be successfully visualized for the first time using the resulting real-case model. These diffusion profiles were then employed to comprehensively evaluate the mechanism of the strip-type sensor, which was assumed to be dominated by the substrate diffusion rate.

Methods

Model geometry

The simulations were performed using the COMSOL® Multiphysics v. 5.6 FEM software package. One- and two-dimensional model geometries were used in this study (Fig. 1). The electrode was set to have a thickness and width of 1 μm and 1 mm, respectively. The sample chamber height was set to 150 μm. These values were selected to match the measurements of the experimental glucose sensor strip.[6] As concentrations are expected to vary more rapidly in the vicinity of the electrode than farther away from it, the finite element mesh was refined at the electrode–solution interface (Fig. 1c).

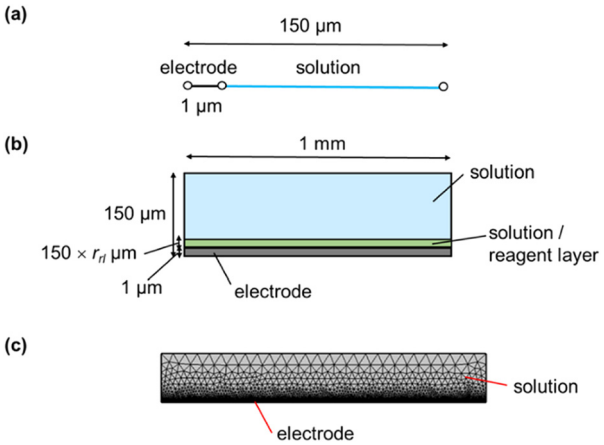

Fig. 1 Simulation model geometry of the glucose sensor strip. (a) Schematic diagram illustrating the one-dimensional model geometry. (b) Schematic diagram illustrating the two-dimensional model geometry with an optional reagent layer. r_{rl} represents the fraction of the solution layer assigned as the reagent layer. (c) Proportional two-dimensional model geometry with a mesh.

Equations and parameters

Unless otherwise stated, the conditions, equations, and parameters adopted for the model are as described previously.[14] Briefly, FAD-GDH follows a ping-pong bi–bi mechanism according to reactions (R1) and (R2). The electrode reaction is described by reaction (R3), where E_O and E_R are the oxidized and reduced FAD-GDH, respectively; M_O and M_R are the oxidized and reduced mediator, respectively; S is glucose; P is gluconolactone; ES is the FAD-GDH bound to glucose; EM is the FAD-GDH bound to the mediator; and k_i is the corresponding reaction rate constant.

$$E_O + S \underset{k_{-1}}{\overset{k_1}{\rightleftharpoons}} ES \overset{k_2}{\rightarrow} E_R + P, \quad \text{(R1)}$$

$$E_R + M_O \underset{k_{-3}}{\overset{k_3}{\rightleftharpoons}} EM \overset{k_4}{\rightarrow} E_O + M_R, \quad \text{(R2)}$$

$$M_R \underset{-k_0}{\overset{k_0}{\rightleftharpoons}} M_O + 2e^-. \quad \text{(R3)}$$

Each species was assigned a diffusion coefficient and was assumed to diffuse in the solution according to Fick's law. The electrode reaction was assumed to follow the Butler–Volmer reaction. Table 1 lists the parameter values used in this study. Although some values were obtained from the literature, numerous were estimated based on fitting.

Table 1 Parameters used in this study

Parameter	Symbol/unit	Value	Ref.
Mediator diffusion coefficient	D_M/cm^2 s^{-1}	2.0×10^{-5}	This study (fitted)
Glucose diffusion coefficient	D_S/cm^2 s^{-1}	6.3×10^{-6}	16[a]
Enzyme diffusion coefficient	D_E/cm^2 s^{-1}	1.0×10^{-11}	14[b]
Mediator standard redox potential	E^0/V	−0.07	6
Double layer capacitance	C_{dl}/μF cm^2	20	14[b]
Electrode conductivity	σ_s/S m^{-1}	4.2×10^7	17
Electrolyte conductivity	σ_l/S m^{-1}	1	15[b]
Symmetry factor	β/-	0.3	This study (fitted)
Enzymatic reaction rate constant	k_1/m^3 s^{-1} mol^{-1}	30	This study (estimated)[c]
Enzymatic reaction rate constant	k_{-1}/s^{-1}	0.3	This study (estimated)[c]
Enzymatic reaction rate constant	k_2/s^{-1}	3000	This study (estimated)[c]
Enzymatic reaction rate constant	k_3/m^3 s^{-1} mol^{-1}	60 000	This study (estimated)[c]
Enzymatic reaction rate constant	k_{-3}/s^{-1}	600	This study (estimated)[c]
Enzymatic reaction rate constant	k_4/s^{-1}	3000	This study (calculated)[c]
Heterogenous rate constant	k_0/cm s^{-1}	8.5×10^{-4}	This study (fitted)
Temperature	T/K	300	14[b]
Initial E_O concentration	cE_init/mM	0.008	This study (set)
Initial M_R concentration	cM_init/mM	0.1	This study (set)

[a] Average value in the reference. [b] Representative value used in previous studies. [c] Values found in the literature and additional assumptions.

Determination of the electrode reaction and mediator diffusion parameters

The electrode reaction and mediator parameters were fitted by varying the target values and subsequently comparing the simulation and experimental results. The simulations were performed using a slightly modified one-dimensional geometry with a total length of 5 mm and electrode thickness of 10 μm, representing the batch-type setup of the corresponding experiment. This batch-type geometry differed significantly in size from the strip-type geometry used in the remainder of this study, with the latter depicted in Fig. 1. The mediator concentration was set to 100 μM and the enzyme and substrate concentrations were set to 0 mM. A triangular wave was set as the electrode potential with a range of 0.5 to −0.3 V and slope of 20 mV s^{-1}. The experiments were performed using a rod electrode in a phosphate buffer solution (pH 7.0) containing 100 μM quinoline-5,8-dione (QD). QD was synthesized as previously reported.[6] Cyclic voltammetry was conducted in the range of 0.5 to −0.3 V at a scan rate of 20 mV s^{-1}.

Determination of the enzymatic reaction parameters

An experimental cyclic voltammogram was obtained using a sensor strip containing 0.1 mM QD and 0.008 mM FAD-GDH with 22.2 mM glucose in phosphate buffer (pH 7.0) to assess the enzymatic reaction parameters. Cyclic voltammetry was performed at −0.5 to 0.5 V at a scan rate of 20 mV s^{-1}.

The values of the enzymatic reaction rate constants k_1–k_4 were estimated using eqn (E1)–(E3).[14]

$$k_{cat} = \frac{k_2 k_4}{k_2 + k_4}, \quad \text{(E1)}$$

$$K_{MS} = \frac{k_4(k_{-1} + k_2)}{k_1(k_2 + k_4)}, \quad \text{(E2)}$$

$$K_{MM} = \frac{k_2(k_{-3} + k_4)}{k_3(k_2 + k_4)}, \quad \text{(E3)}$$

where k_{cat} is the catalytic turnover number, K_{MS} is the Michaelis–Menten constant of the enzyme with the substrate, and K_{MM} is the Michaelis–Menten constant of the enzyme with the mediator. The following numerical values were obtained from the literature: k_{cat} = 1500 s^{-1},[6] K_{MS} = 50 mM,[10] and K_{MM} = 0.03 mM.[6]

Cyclic voltammetry was simulated using a glucose sensor strip with a one-dimensional geometry (Fig. 1a), 0.1 mM of mediator, 0.008 mM of enzyme, and 22.2 mM of substrate. The electrode potential was a triangular wave with a range and slope of −0.5 to 0.5 V and 20 mV s^{-1}, respectively.

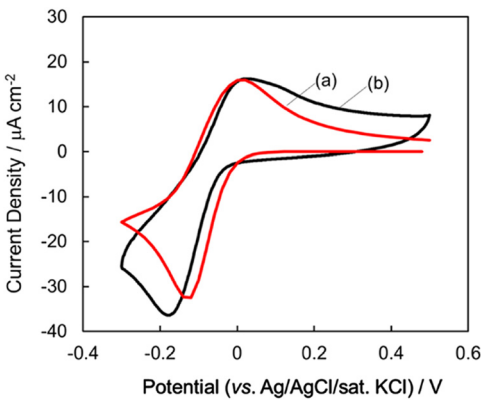

Fig. 2 (a) Simulated and (b) experimental cyclic voltammograms. Scan rate: 20 mV s^{-1}. (a) Conditions: 100 μM mediator, k_0 = 8.5 × 10^{-4} cm s^{-1}, β = 0.3, and D_M = 2.0 × 10^{-5} cm^2 s^{-1}. (b) Conditions: 100 μM QD and phosphate buffer (pH 7.0).

Results and discussion

Simulation to determine specific parameter values

Unknown electrode reaction and mediator parameters, such as the heterogeneous electron transfer constant (k_0), symmetry factor (β), and mediator diffusion coefficient (D_M), were determined by fitting the simulated cyclic voltammograms to an experimental QD voltammogram obtained *via* a batch-type measurement (Fig. 2). The influence of each of the three parameters on the shape of the cyclic voltammogram is described here to compare the simulated voltammograms for two distinct values with all other parameters set to the same values (Fig. S1–S3).

The simulated voltammogram resembled the experimental voltammogram most at $k_0 = 8.5 \times 10^{-4}$ cm s^{-1}, $\beta = 0.3$, and $D_M = 2.0 \times 10^{-5}$ cm^2 s^{-1} (Fig. 2 and Table 1). The peak potential and current density values of the oxidation peaks derived from the simulated and experimental results were in good agreement (Fig. 2). The peak potential and current density values of the reduction peaks were a reasonably good, though slightly poorer, match (Fig. 2). In this study, fitting was performed by manually changing the parameter of interest and comparing the simulation results with the experimental data. Furthermore, although the iR drop effects originating from the solution resistance and first 10 μm of the working electrode were considered, those from other parts of the experimental system were not. Additionally, identical k_0 and D_M values were used for the oxidized and reduced mediator. However, the k_0 and D_M values can differ slightly between oxidized and reduced species, which might have led to the slightly poorer match of the reduction peaks. However, these parameter values were used for all subsequent simulations in this study (Table 1).

Enzymatic reaction rate constants k_1–k_4 were estimated from the known k_{cat} and K_M values. This study assumed that once the reactants are bound to the enzyme, the oxidation and reduction reaction rates are equal, that is, $k_2 = k_4$ ((R1), (R2)). tfgap reactants binding to the enzyme was assumed to be 100-fold faster than the corresponding reverse reaction, that is, $k_1 = k_{-1} \times 100$ [m^3 mol^{-1}] (R1) and $k_3 = k_{-3} \times 100$ [m^3 mol^{-1}] (R2). Given these conditions, eqn (E1)–(E3), $k_{cat} = 1500$ s^{-1},[6] $K_{MS} = 50$ mM,[10] and $K_{MM} = 0.03$ mM,[6] the enzymatic reaction rate constants were estimated to be $k_1 = 30$ m^3 s^{-1} mol^{-1}, $k_{-1} = 0.3$ s^{-1}, $k_2 = 3000$ s^{-1}, $k_3 = 60\,000$ m^3 s^{-1} mol^{-1}, $k_{-3} = 600$ s^{-1}, and $k_4 = 3000$ s^{-1} (Table 1). Employing these reaction rate constants for the simulation resulted in reasonably well matched simulated and experimental voltammograms (Fig. 3). The remaining differences in the voltammograms can be attributed to the differences between the estimated and actual kinetic parameters derived from the restrictions placed on the estimation. While the assumptions made were both reasonable and necessary for determining the rate constant, they consequently increased the uncertainty of the estimation. Additionally, the simulation does not account for the fact that FAD-GDH only reacts with the β-anomer of glucose. However, the onset potentials and diffusion-limited current densities of the simulated and experimental results were similar. Therefore, these reaction rate constants were considered sufficiently accurate.

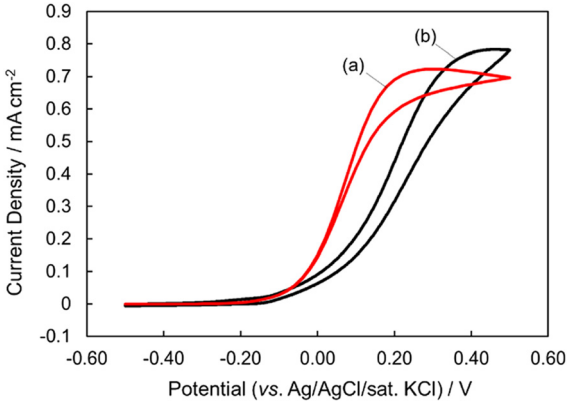

Fig. 3 (a) Simulated and (b) experimental cyclic voltammograms. Scan rate: 20 mV s^{-1}. (a) Conditions: 22.2 mM substrate, 0.008 mM enzyme, 0.1 mM mediator, $k_1 = 30$ m^3 s^{-1} mol^{-1}, $k_{-1} = 0.3$ s^{-1}, $k_2 = 3000$ s^{-1}, $k_3 = 60\,000$ m^3 s^{-1} mol^{-1}, $k_{-3} = 600$ s^{-1}, and $k_4 = 3000$ s^{-1}. (b) Conditions: 22.2 mM glucose, 0.008 mM FAD-GDH, 0.1 mM QD, and phosphate buffer (pH 7.0).

Simulation of a glucose sensor strip with homogeneously dissolved reactants

Chronoamperometry simulations (Fig. 4a) were performed using a glucose sensor strip with a two-dimensional geometry (Fig. 1b) and the determined parameter values (Table 1). The substrate, mediator, and enzyme were initially homogeneously distributed in the solution domain.

The simulated chronoamperogram (Fig. 4a) shows an initial rapid decrease in current, which can be attributed to

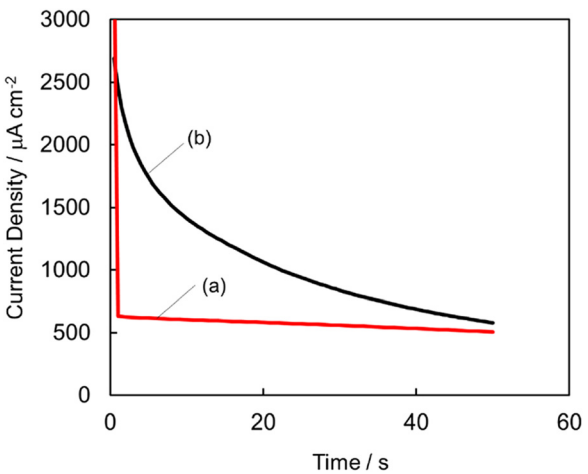

Fig. 4 (a) Simulated and (b) experimental chronoamperograms of the glucose sensor strip. Applied potential: 0.3 V. (a) Conditions: 22.2 mM substrate, 0.008 mM enzyme, 0.1 mM mediator, and homogeneous distribution in the entire solution domain. (b) Conditions: 22.2 mM glucose, 0.008 mM FAD-GDH, 0.1 mM QD, and phosphate buffer (pH 7.0).

the charging of the electric double layer. This trend is followed by a relatively stable steady-state current. In contrast, the corresponding experimental chronoamperogram (Fig. 4b) shows a slow decrease in the current. This clear difference between the simulated and experimental results suggests that a significant factor has not yet been considered in the simulation.

Simulation of a glucose sensor strip with an initial reactant layer

One obvious, yet often overlooked, difference between simulations and experiments is the "location" of the mediator and enzyme. In the above simulations, the substrate, mediator, and enzyme were homogeneously distributed throughout the entire solution domain. In the glucose sensor strip experiment, the mediator and enzyme were dried on the electrode and began dissolving and diffusing into the solution upon contact with the glucose solution.

Glucose sensor strips were simulated with the enzyme and mediator initially limited to the electrode surface to mimic this process. Accordingly, a reagent layer domain was defined to cover a fraction (r_{rl}) of the solution domain on top of the electrode (Fig. 1b). The enzyme and mediator concentrations in the reagent layer domain were initially set to $1/r_{rl}$ times the target value, while that of the remaining solution domain was set to zero. At the beginning of the simulation, the enzyme and mediator could diffuse throughout the entire solution domain. The substrate was initially set as homogeneously distributed at the target concentration.

The chronoamperogram simulated with the model containing a reagent layer with r_{rl} = 1/10 closely matched the experimental data (Fig. 5). This result indicates that the enzyme and mediator may not be homogeneously distributed at the beginning of measurement; instead, they may be concentrated closer to the electrode surface.

The simulation was conducted using various glucose concentrations (Fig. S4). The simulated current density at 10 s matched the experimental data (Fig. S4b[6]).

The enzyme and mediator in this type of biosensor are often assumed to dissolve completely before the start of measurement; however, little to no investigations have been performed to confirm this assumption. Further investigations are necessary to determine whether the incomplete dissolution observed in this study is common or an exception.

Notably, this type of biosensor operates with a very small sample volume. This may result in the excessively rapid consumption of the analyte to achieve a pseudo-steady state, which is not problematic provided that measurements are conducted at a specific, tightly controlled time point after the start of potential application.

Concentration distribution profiles

A major advantage of two-dimensional simulations is the availability of concentration distribution profiles (Fig. 6, 7, and S5). The reaction progress and rate-limiting diffusion process can be determined using the concentration distribution profiles obtained at different time points.

In the case of the glucose sensor strip with a reactant layer, the reduced mediator is initially present only in the reactant layer (Fig. 6a and b, 0 s). The reduced mediator diffuses quickly into and remains homogeneously distributed throughout the solution, except in the vicinity of the electrode (Fig. 6a and b, 10–50 s). The oxidized mediator is only present in the vicinity of the electrode (Fig. S5). That is, a very thin concentration gradient and, thus, a very thin

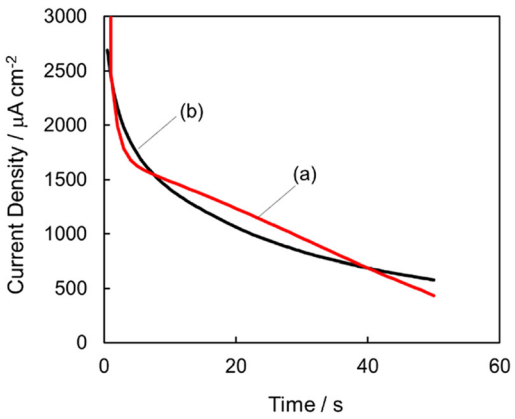

Fig. 5 (a) Simulated and (b) experimental chronoamperograms of the glucose sensor strip. Applied potential: 0.3 V. (a) Conditions: entire solution domain, 22.2 mM substrate; reagent layer domain (r_{rl}), 1/10; 0.08 mM enzyme; and 1 mM mediator. (b) Conditions: 22.2 mM glucose, 0.008 mM FAD-GDH, 0.1 mM QD, and phosphate buffer (pH 7.0).

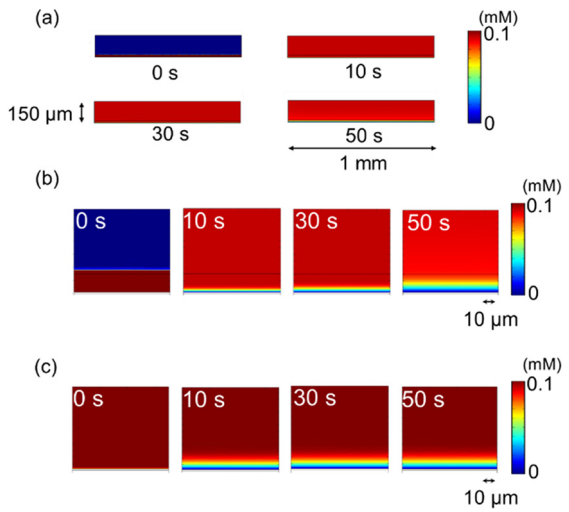

Fig. 6 Concentration distribution profiles of the reduced mediator over 0, 10, 30, and 50 s of chronoamperometry (a and b) with and (c) without the reactant layer. (a) Overall view and (b and c) magnified view near the electrode.

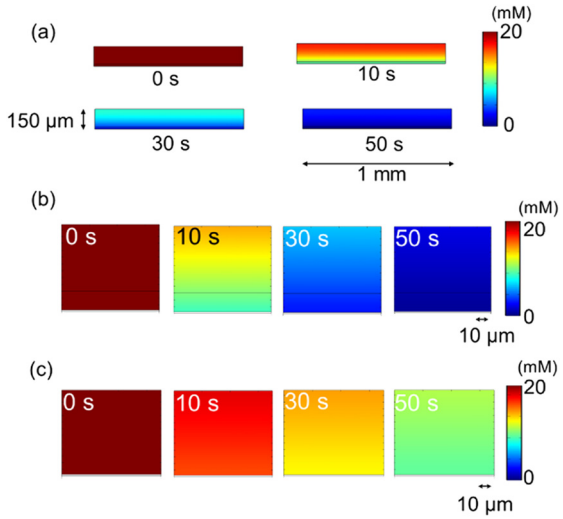

Fig. 7 Concentration distribution profiles of the substrate over 0, 10, 30, and 50 s of chronoamperometry (a and b) with and (c) without the reactant layer. (a) Overall view and (b and c) magnified view near the electrode.

diffusion layer, is formed and maintained for the mediator, with the reduced mediator diffusing toward the electrode and the oxidized mediator diffusing toward the solution. In contrast, the substrate is initially homogeneously distributed throughout the solution (Fig. 7a and b, 0 s), gradually forming a concentration gradient and diffusion layer spanning the entire solution domain (Fig. 7a and b, 10–50 s).

Interestingly, except for the initial diffusion, the mediator and substrate behave similarly even without the reagent layer (Fig. 6c and 7c). The reduced mediator in the vicinity of the electrode is rapidly oxidized, forming a thin reduced mediator concentration gradient (Fig. 6c). The diffusion gradient of the substrate spans the entire solution domain (Fig. 7c). Compared with the system with a reagent layer, the formation of the reduced mediator concentration gradient is faster, while the depletion of the total substrate concentration is slower. These timescale differences can be attributed to the differences in the local reactant concentrations.

Notably, the initial mediator and enzyme distributions in the experimental glucose sensor strip is likely intermediate between a homogeneous distribution and localization within the reagent layer. The mediator and enzyme are dissolved from a dry layer by the influx of sample. This sample influx initially creates a convection force within the solution, which is not considered in the present simulation model. However, the above results indicate that the mediator oxidized at the electrode is immediately reduced by the enzyme at a location close to the electrode. Therefore, mediator diffusion exerts little to no influence on the total reaction rate of the glucose sensor strip. However, the substrate diffuses over a longer distance from the bulk to the electrode before it reacts with the enzyme. Therefore, substrate diffusion controls the total reaction rate of glucose sensor strips with QD as a mediator. Notably, as with all enzymatic biosensors, the reaction rate of the sensor strips at high glucose concentrations becomes limited by the enzyme kinetics. This finding agrees with the results of a previous experimental investigation.[6] That is, by adapting a general simulation model for mediator-type enzyme electrodes[14] to model a specific glucose sensor strip[6] enables both the visualization of the internal state of the sensor strip at various time points and confirms the rate-limiting step of the reaction.

Conclusion

In this study, a general FEM simulation model for mediator-type enzyme electrodes was adapted into a model for a glucose sensor strip with QD as the mediator. Several key parameters were determined by fitting the simulated cyclic voltammograms to the corresponding experimental ones. The simulated chronoamperograms suggested that the enzyme and mediator in the glucose sensor strip are not instantly homogeneously distributed in the solution, as is commonly assumed, but are initially concentrated in the vicinity of the electrode. Furthermore, the simulated concentration distribution profiles confirmed that the mediator forms a very thin diffusion layer on top of the electrode while the substrate diffuses throughout the solution. These findings confirm that the total reaction rate of the glucose sensor strip with QD as the mediator is limited by the substrate diffusion rate. Notably, as with other mediators, the limiting factor may be a mixture of substrate and mediator diffusion. The simulation model and method of adaptation used in this study can be applied to the screening of new mediators for sensor strips with a substrate diffusion-limited reaction rate. The results of this study generally demonstrate the usefulness of an adapted simulation model to obtain an improved understanding of the mechanism of specific biosensors.

Author contributions

I. S. and S. T. conceptualized the study. M. M. and N. L. conducted the simulations. M. M. performed the electrochemical experiments. M. M. and N. L. drafted the initial version of the manuscript. I. S. and N. L. revised and finalized the manuscript. I. S., H. W., M. I., and S. T. supervised the work.

Conflicts of interest

The authors declare no conflicts of interest.

Data availability

Supplementary information is available. See DOI: **https://doi.org/10.1039/D5SD00095E**.

All data supporting the findings of this study are included within the article and its supplementary information files.

The data supporting this study are available from the corresponding author upon reasonable request.

References

1 R. Bernstein, J. L. Parkes, A. Goldy, D. Brown, B. Harrison, A. Chu, B. K. Pflug, D. A. Simmons, S. Pardo and T. S. Bailey, A new test strip technology platform for self-monitoring of blood glucose, *J. Diabetes Sci. Technol.*, 2013, **7**, 1386–1399, DOI: **10.1177/193229681300700531**.

2 A. Heller and B. Feldman, Electrochemical glucose sensors and their applications in diabetes management, *Chem. Rev.*, 2008, **108**, 2482–2505, DOI: **10.1021/cr068069y**.

3 K. Benkhadra, F. Alahdab, S. Tamhane, Z. Wang, L. J. Prokop, I. B. Hirsch, D. Raccah, J.-P. Riveline, O. Kordonouri and M. H. Murad, Real-time continuous glucose monitoring in type 1 diabetes: A systematic review and individual patient data meta-analysis, *Clin. Endocrinol.*, 2017, **86**, 354–360, DOI: **10.1111/cen.13290**.

4 A. Heller and B. Feldman, Electrochemistry in diabetes management, *Acc. Chem. Res.*, 2010, **43**, 963–973, DOI: **10.1021/ar9002015**.

5 H. Teymourian, A. Barfidokht and J. Wang, Electrochemical glucose sensors in diabetes management: An updated review (2010–2020), *Chem. Soc. Rev.*, 2020, **49**, 7671–7709, DOI: **10.1039/D0CS00304B**.

6 J. Morshed, R. Nakagawa, M. M. Hossain, Y. Nishina and S. Tsujimura, Disposable electrochemical glucose sensor based on water-soluble quinone-based mediators with flavin adenine dinucleotide-dependent glucose dehydrogenase, *Biosens. Bioelectron.*, 2021, **189**, 113357, DOI: **10.1016/j.bios.2021.113357**.

7 R. Bennett, E. Blochouse and D. Leech, Effect of individual plasma components on the performance of a glucose enzyme electrode based on redox polymer mediation of a flavin adenine dinucleotide-dependent glucose dehydrogenase, *Electrochim. Acta*, 2019, **302**, 270–276, DOI: **10.1016/j.electacta.2019.02.039**.

8 J. Okuda-Shimazaki, H. Yoshida and K. Sode, FAD dependent glucose dehydrogenases – Discovery and engineering of representative glucose sensing enzymes, *Bioelectrochem.*, 2020, **132**, 107414, DOI: **10.1016/j.bioelechem.2019.107414**.

9 S. Tsujimura, From fundamentals to applications of bioelectrocatalysis: Bioelectrocatalytic reactions of FAD-dependent glucose dehydrogenase and bilirubin oxidase, *Biosci., Biotechnol., Biochem.*, 2019, **83**, 39–48, DOI: **10.1080/09168451.2018.1527209**.

10 S. Tsujimura, S. Kojima, K. Kano, T. Ikeda, M. Sato, H. Sanada and H. Omura, Novel FAD-dependent glucose dehydrogenase for a dioxygen-insensitive glucose biosensor, *Biosci., Biotechnol., Biochem.*, 2006, **70**, 654–659, DOI: **10.1271/bbb.70.654**.

11 S. Ferri, K. Kojima and K. Sode, Review of glucose oxidases and glucose dehydrogenases: A bird's eye view of glucose sensing enzymes, *J. Diabetes Sci. Technol.*, 2011, **5**, 1068–1076, DOI: **10.1177/193229681100500507**.

12 E.-H. Yoo and S.-Y. Lee, Glucose biosensors: An overview of use in clinical practice, *Sens.*, 2010, **10**, 4558–4576, DOI: **10.3390/s100504558**.

13 Y. Kitazumi, T. Noda, O. Shirai, M. Yamamoto and K. Kano, Characteristics of fast mediated bioelectrocatalytic reaction near microelectrodes, *Phys. Chem. Chem. Phys.*, 2014, **16**, 8905–8910, DOI: **10.1039/C4CP00141A**.

14 N. Loew, T. Ofuji, I. Shitanda, Y. Hoshi, Y. Kitazumi, K. Kano and M. Itagaki, Cyclic voltammetry and electrochemical impedance simulations of the mediator-type enzyme electrode reaction using finite element method, *Electrochim. Acta*, 2021, **367**, 137483, DOI: **10.1016/j.electacta.2020.137483**.

15 N. Loew, H. Watanabe, I. Shitanda and M. Itagaki, Electrochemical impedance spectroscopy: Simultaneous detection of different diffusion behaviors as seen in finite element method simulations of mediator-type enzyme electrodes, *Electrochim. Acta*, 2022, **421**, 140467, DOI: **10.1016/j.electacta.2022.140467**.

16 S. Miyamoto, K. Atsuyama, K. Ekino and T. Shin, Estimating the diffusion coefficients of sugars using diffusion experiments in agar-gel and computer simulations, *Chem. Pharm. Bull.*, 2018, **66**, 632–636, DOI: **10.1248/cpb.c18-00071**.

17 T. Honda, Application of the electrically conductive ink for electronics components, *Nippon Insatsu Gakkaishi*, 2003, **40**, 24–32, DOI: **10.11413/nig1987.40.24**.